

# A unified model of the dynamics and spectroscopy of the $g^3\Sigma_0^-$ and $E^1\Sigma^+$ states of hydrogen chloride

Alex Strizhev, Xiaonong Li, Rohana Liyanage,<sup>a)</sup> and Robert J. Gordon  
Department of Chemistry (m/c 111), University of Illinois at Chicago, 845 West Taylor Street, Chicago,  
Illinois 60607-7061

Robert W. Field  
Department of Chemistry (6-219), Massachusetts Institute of Technology, Cambridge, Massachusetts 02139

(Received 28 August 1997; accepted 7 October 1997)

The yield,  $Y$ , the spin-orbit branching ratio,  $\Gamma$ , and the angular anisotropy,  $\beta_2$ , of Cl atoms produced by predissociation of the  $E^1\Sigma^+$  and  $g^3\Sigma_0^-$  Rydberg states of HCl and DCl are reported as functions of the rotational angular momentum  $J$ . For the  $E$  state,  $Y$  increases with  $J$  for HCl and decreases with  $J$  for DCl, whereas  $\Gamma$  and  $\beta_2$  are independent of  $J$  for both isotopomers. For the  $g_0$  state  $Y$  increases with  $J$ , whereas  $\Gamma$  and  $\beta_2$  both decrease with  $J$  for both isotopomers. The different dynamical behavior of these two  $0^+$ -symmetry states belonging to the same zero-order electronic configuration is explained in terms of their diabatic characters. © 1998 American Institute of Physics. [S0021-9606(98)00503-0]

## INTRODUCTION

The diabatic model is a powerful tool for interpreting the electronic spectra of molecules. The central assumption of this model is that an effective, zero-order Hamiltonian describes the essential properties of the electronic states of a molecule, and that the complexity observed in its spectrum is caused by perturbations arising from terms omitted from that Hamiltonian. These perturbations, such as the spin-orbit, rotational, and electrostatic interactions, are readily expressed in terms of a small number of molecular parameters, which can be used to represent and explain diverse spectroscopic effects such as  $\Lambda$ -doubling and intensity anomalies.<sup>1</sup> The central point of this paper is that the same deperturbation techniques used to interpret the molecular spectrum can also explain the *dynamical* behavior of a molecule.

Here, we present data on several aspects of the photodissociation dynamics of the  $g^3\Sigma_0^-$  and  $E^1\Sigma^+$  Rydberg states of HCl and DCl.<sup>2-4</sup> These states are interesting because they have the same nominal electronic structures, namely a  $4p\pi$  Rydberg electron bound to a  $^2\Pi_{3/2}$  ionic core, but very different spectroscopic properties. Our goal is to show how the distinct diabatic characters of these states can be used to interpret their dynamics. In previous papers we reported intensity anomalies in the resonance-enhanced multiphoton ionization (REMPI) spectra of the  $E^1\Sigma^+ \leftarrow X^1\Sigma^+$  transition of HCl and DCl,<sup>3</sup> and the Cl spin-orbit branching ratio for the predissociation of the  $g^3\Sigma_0^-$  state of HCl.<sup>4</sup> In the present paper we extend our dynamical studies of these states and compare their behavior systematically. Other states belonging to the same Rydberg complex are the  $e^3\Sigma^+$ ,  $G^1\Sigma^-$ ,  $F^1\Delta$ , and  $f^3\Delta$  states. The spectroscopy and dynamics of the last two states were explored in previous publications.<sup>3,5,6</sup>

## EXPERIMENTAL METHODS AND RESULTS

The experimental methods have been described previously.<sup>6</sup> Briefly, two counterpropagating excimer-pumped pump and probe dye lasers are used to excite HCl (or DCl) molecules and to probe their fragments. Two photons from the first laser transfer population to a Rydberg state, which either predissociates to yield ground state H and Cl( $^2P_i$ ) atoms or absorbs a third photon to reach a superexcited state. The latter can either autoionize to produce HCl<sup>+</sup> (or DCl<sup>+</sup>) or (pre)dissociate to yield one excited and one ground state atom. The excited atoms (but not the ground state atoms) are subsequently ionized by the pump laser. The second laser is used to detect the ground state  $^{35}\text{Cl}$  fragment atoms, again by 2 + 1 REMPI.<sup>7</sup> The experiment is performed in a vacuum chamber filled with  $\sim 2 \times 10^{-5}$  Torr of HCl or DCl. The product ions are detected by time-of-flight mass spectroscopy, using Wiley-McLaren<sup>8</sup> electrodes, a micro-channel plate detector, and a boxcar signal averager.

Two types of measurements are performed. In the first experiment the spin-orbit branching ratio of the fragment ground state ( $3p^5\ ^2P_i$ ) Cl atom is measured as a function of rotational quantum number  $J$  of the parent molecule. A delay of 50 ns is introduced between the pump and probe lasers to distinguish between Cl<sup>+</sup> produced by the pump or by the probe laser. The laser jitter in both experiments is  $\pm 10$  ns. The pump laser is tuned to different  $Q$ -branch lines of either the  $g^3\Sigma_0^- \leftarrow X^1\Sigma^+$  or the  $E^1\Sigma^+ \leftarrow X^1\Sigma^+$  (0-0) transition, and the probe laser is tuned alternately to the Cl( $4p\ ^2D_{3/2}$ )  $\leftarrow$  Cl( $3p^5\ ^2P_{3/2}$ ) transition centered at 235.338 nm or to the Cl( $4p\ ^2P_{1/2}$ )  $\leftarrow$  Cl( $3p^5\ ^2P_{1/2}$ ) transition at 235.204 nm. The relative yield,

$$Y \propto \frac{[\text{Cl}_{1/2}] + [\text{Cl}_{3/2}]}{[\text{HCl}^+]}, \quad (1)$$

and the branching ratio

<sup>a)</sup>Present address: Department of Chemistry, University of Utah, Salt Lake City, UT 84112.

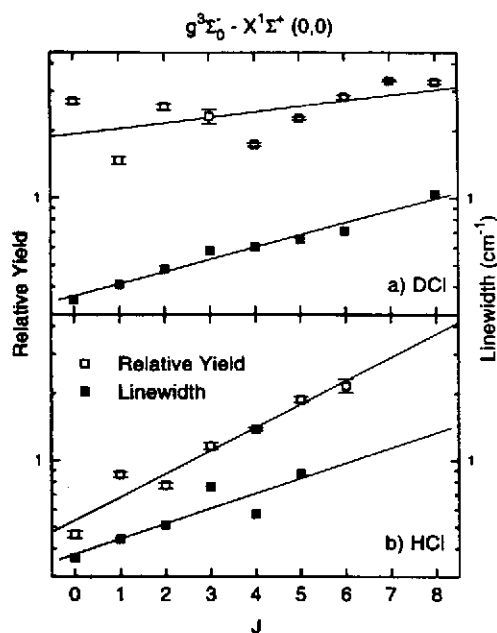


FIG. 1. Linewidths and dissociation yields for the  $g^3\Sigma_0^- - X^1\Sigma^+$  (0-0) transition of (a) DCl and (b) HCl. The straight lines are linear least-squares fits included to guide the eye.

$$\Gamma = \frac{[Cl_{1/2}]}{[Cl_{1/2}] + [Cl_{3/2}]}, \quad (2)$$

are determined from the pump ( $HCl^+$ ) and probe ( $Cl_{1/2}^+$  and  $Cl_{3/2}^+$ ) signals. In the yield measurements the relative intensities of the atomic and molecular ion signals were not calibrated, whereas for the branching ratio the relative ionization efficiency factor derived from the data of Wittig *et al.*<sup>9,10</sup> was used. The yields for the  $g_0$  state are plotted in Fig. 1 along with the linewidths of the parent ion signal. Previously<sup>3</sup> we reported intensity anomalies of the  $E$  state, which are proportional to  $Y$ . The branching ratios for both the  $E$  and  $g_0$  states are shown in Fig. 2. In an earlier study<sup>4</sup> we reported a value of  $\Gamma = 1$  for the  $g_0(J=1)$  state of HCl; however, re-measurement of the branching ratio for this state revealed a small  $Cl(^2P_{3/2})$  yield that was previously undetected.

In the second experiment the angular anisotropy of the recoiling atoms is measured using the method of velocity aligned Doppler spectroscopy (VADS).<sup>11,12</sup> Again, only Q-branch transitions are studied. In this case the delay between the two lasers is set at 60 ns. The etalon narrowed probe laser, with a nominal bandwidth of  $0.04 \text{ cm}^{-1}$  of the dye fundamental, scans the  $Cl(4p^2D_{3/2}) \leftarrow Cl(3p^5^2P_{3/2})$  transition for each pumped state. The results for DCl are shown in Fig. 3 for the  $g_0$  state and in Fig. 4 for the  $E$  state. Similar data for HCl obtained over a narrower range of  $J$  values ( $J=1-5$  for the  $g_0$  state and  $J=2-3$  for the  $E$  state) are plotted in Figs. 5 and 4, respectively.

## DISCUSSION

The data show a number of striking differences between the dynamics of the  $g_0$  and  $E$  states. Figure 1 shows that the

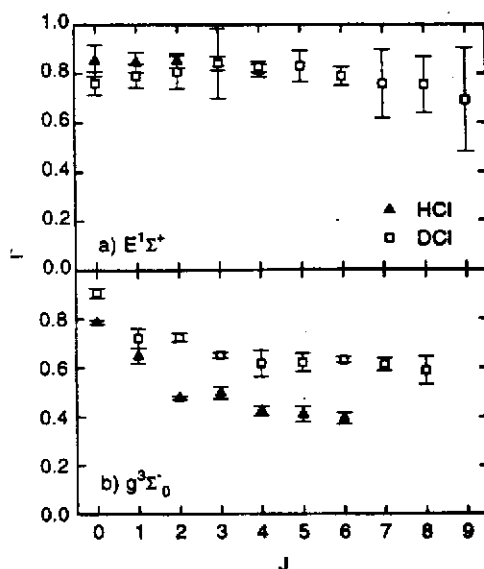


FIG. 2. Spin-orbit branching ratios ( $\Gamma$ ) of the Cl fragment for (a) the  $E^1\Sigma^+ - X^1\Sigma^+$  (0-0) and (b) the  $g^3\Sigma_0^- - X^1\Sigma^+$  (0-0) transition. Solid points are for HCl and open points are for DCl. Error bars are one standard deviation.

predissociation yields of the  $g_0$  states of both HCl and DCl increase with  $J$ , whereas previously<sup>3</sup> we found that for the  $E$  state the yield increases with  $J$  for HCl and decreases for DCl. Although both the  $g_0$  and  $E$  states have  $\Gamma$  values (Fig. 2) larger than the statistical ratio of  $1/3$ , for the  $E$  state this ratio is nearly independent of  $J$ , whereas for  $g_0$  it decreases with  $J$ . There is a similar  $g_0$  vs  $E$  dichotomy for the Doppler profiles (Figs. 3-5). Both states have Doppler profiles with a maximum at the center for  $J=1$  (the lowest  $J$  measured). For the  $g_0$  state, however, the Doppler profiles are increasingly split at higher  $J$ . Since the polarization vector of the pump laser is perpendicular to the propagation direction of the probe laser, an unsplit Doppler profile indicates that the fragments recoil along an axis parallel to the transition dipole vector, whereas a split profile indicates that the recoil is perpendicular to the transition dipole vector.

A key factor for understanding the disparate behavior of these two states is the recoil energy of the fragments. The molecule may dissociate after absorbing either two or three photons. Because one of the fragments from the three-photon ( $3\omega$ ) process is electronically excited ( $E=82\,303 \text{ cm}^{-1}$  for  $H(n=2)$  or  $74\,221 \text{ cm}^{-1}$  for  $Cl(4s^2P_{3/2})$ , which is larger than the one-photon energy of  $41\,544 \text{ cm}^{-1}$  for the  $g_0$  state) the recoil velocity for this case is much smaller than for the two-photon ( $2\omega$ ) process. Ground state  $Cl(3p^5^2P_i)$  atoms originating from a  $3\omega$  process can be produced either as the partner of the  $H(n=2)$  fragment ("the  $H^*$  channel") or as the result of fluorescent decay of an excited Cl fragment ("the  $Cl^*$  channel"). For both the  $g_0$  and  $E$  states, we observed an  $H^+$  signal produced by the pump laser, presumably by nonresonant ionization of  $H(n=2)$ . This observation proves that at least some of the Cl atoms detected by the probe laser are produced by the  $H^*$  channel.

A quantitative measure of the recoil velocity  $v$  can be

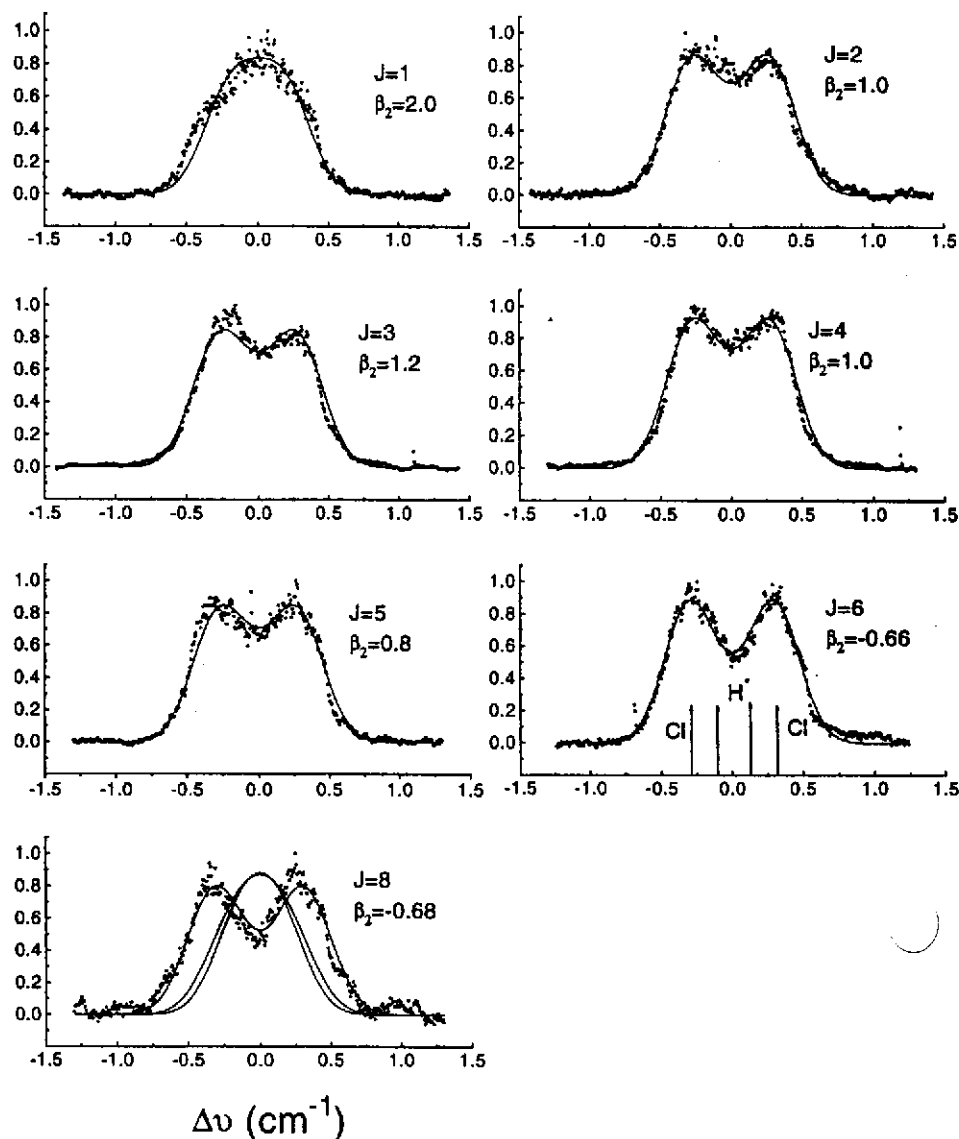


FIG. 3. Doppler profiles of  $\text{Cl}(^2P_{3/2})$  produced by predissociation of the  $g^3\Sigma_0^-$  state of  $\text{DCl}$ . The smooth curves and the  $\beta_2$  values were obtained by the fitting method described in the text, assuming a two-photon mechanism. Also shown for the  $J=8$  data is the simulated profile for the three-photon  $\text{H}^*$  and  $\text{Cl}^*$  mechanisms. The vertical arrows in the  $J=6$  scan indicate the velocities of  $\text{Cl}(^2P_{3/2})$  atoms produced by either two photons (1,313 m/s) or by three photons via the  $\text{H}^*$  channel (479 m/s).

obtained from the Doppler profile,  $D(w/v)$ , where  $w$  is the projection of  $\mathbf{v}$  along the probe direction, and  $v = |\mathbf{v}|$ . For coaxial geometry, the Doppler profile for two-photon excitation is given by<sup>13</sup>

$$D(w/v) = 1 - \frac{1}{2}\beta_2 P_2(w/v) + \frac{3}{8}\beta_4 P_4(w/v), \quad (3)$$

where  $P_s$  are Legendre polynomials, and the anisotropy parameters  $\beta_s$  are functions of the initial and final rotational and electronic quantum numbers. The experimental profile depends also on the resolution of the pump laser,  $\delta\nu$ , and the rms spot size of the two focused lasers,  $\rho$ , which are only approximately known. Compared with the uncertainty in these quantities,  $\beta_4$  has only a minor effect on the shape of the profile, and it is unlikely that higher order anisotropy terms resulting from absorption of three or more photons would have a significant effect in this experiment. Our fitting

procedure was to assume a semiclassical value<sup>13,14</sup> of  $\beta_2 \sim -5/7$  for  $J=6$  and 8 and to determine the instrument parameters ( $\rho = 30 \pm 2 \mu\text{m}$  and  $\delta\nu = 0.21 \pm 0.02 \text{ cm}^{-1}$ ) by a least-squares fit of  $D(w/v)$ . The instrument parameters were assumed to have the same values for lower  $J$ , for which  $\beta_2$  was obtained by a least-squares fit.

The data in Figs. 3 and 5 show a progression from parallel to perpendicular recoil with increasing  $J$ . In the case of perpendicular recoil, the splitting of the VADS peaks provides a direct measure of the fragment velocity, as indicated by the vertical arrows in Fig. 3. For the  $g_0$  state of  $\text{HCl}$  and  $\text{DCl}$ , the observed splitting shows that  $\text{Cl}$  is produced almost exclusively by  $2\omega$ , a result which is confirmed by the least-squares fit of the profile. Further evidence that  $\text{Cl}$  is produced mostly by  $2\omega$  is our observation that the intensity depen-

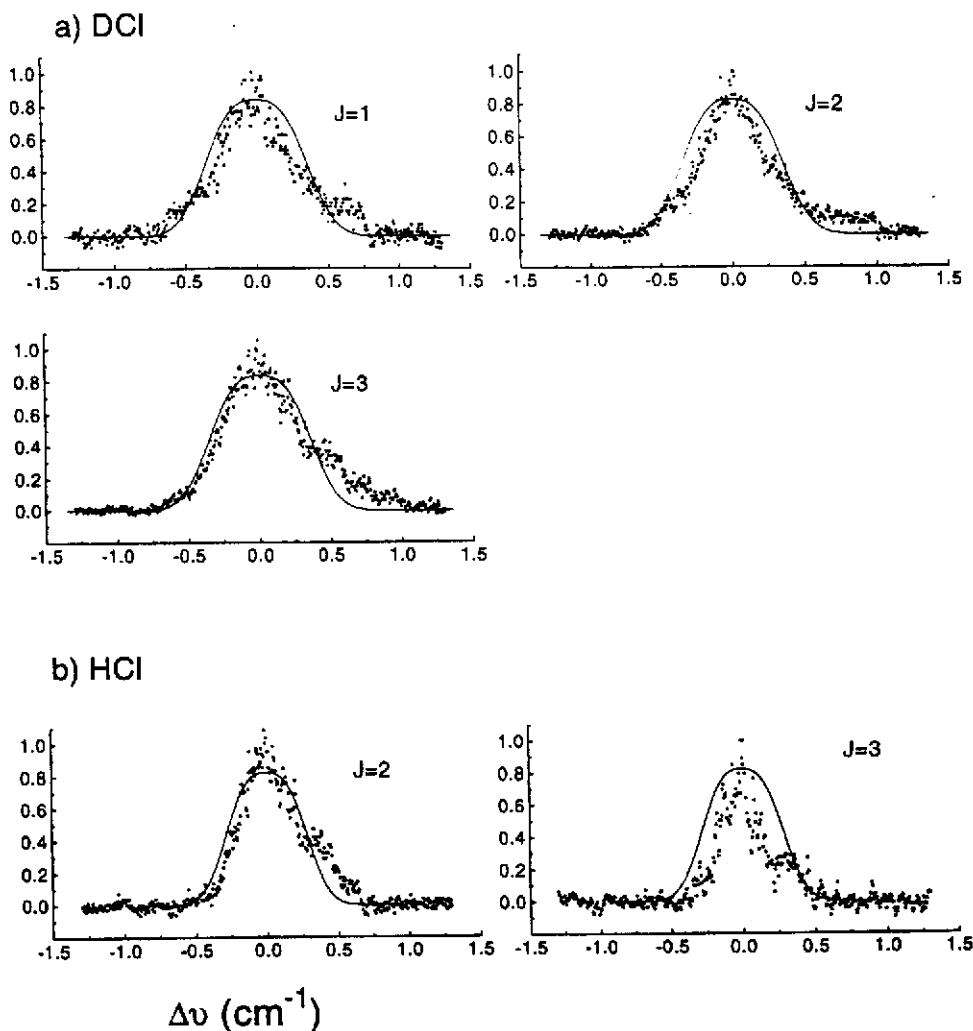


FIG. 4. Doppler profiles of  $\text{Cl}(^2P_{3/2})$  produced by predissociation of the  $E^1\Sigma^+$  state of (a) DCl and (b) HCl. The smooth curves are the fitted Doppler profiles for the  $g^3\Sigma_0^-$  ( $J=1$ ) state, which are shown for comparison.

dence of the  $\text{H}^+$  signal (which necessarily arises from a  $3\omega$  process) has a larger power-law exponent,  $n$ , than that of the  $\text{Cl}^+$  signal produced by the probe laser ( $n=2.1\pm 0.03$  vs  $1.6\pm 0.03$ , both exponents referring to the pump intensity). For the  $E$  state, where there is no VADS splitting,  $D(w/v)$  is  $\sim 10\%$  narrower than for  $g_0(J=1)$  (see Fig. 4), indicating that a significant fraction of the probed Cl atoms are produced by  $3\omega$ .

In an earlier study<sup>3</sup> we showed that the dissociation yield of the  $E$  state is determined by Rydberg-valence mixing of the  $E$  and  $V^1\Sigma^+$  states at the  $2\omega$  level. The mixing coefficients vary with  $J$  and are different for the two isotopomers. The opposite  $J$  dependencies of the intensity anomalies in the REMPI spectra of HCl and DCl are the result of dissociation at the  $3\omega$  level, which is determined by the state character at the  $2\omega$  level.<sup>15</sup> The identity of the predissociating state(s), however, and hence  $\Gamma$ , is independent of  $J$ . The  $J$  independence of  $\beta_2$  for the  $E$  state, at least for the few rotational levels that we examined, is consistent with the fact that the  $E$  and  $V$  states have the same  $0^+$  character.

The  $J$ -dependent dynamics of the  $g_0$  state strongly indicate a rotational perturbation by some state at the  $2\omega$  level. Consider first  $\Gamma$ . We pointed out previously<sup>4</sup> that the preponderance of  $\text{Cl}(3p^2P_{1/2})$  at  $J=0$  could be explained by the fact that the  $e$  symmetry of the  $g^3\Sigma_0^-$  state does not allow it to couple to any of the continuum states other than the  $a^3\Pi_0^+$  state. This continuum state correlates adiabatically<sup>16</sup> with  $\text{Cl}(^2P_{1/2})$  and diabatically<sup>17</sup> with  $2/3 \text{Cl}(^2P_{1/2})$  and  $1/3 \text{Cl}(^2P_{3/2})$ . Our measured values of  $\Gamma=0.91\pm 0.02$  for DCl and  $0.79\pm 0.01$  for HCl lie between these limits. The same argument explains the large value of  $\Gamma$  for the  $E$  state. In the case of the  $g_0$  state, as  $J$  increases, rotational coupling to continuum states that correlate to an excess of  $\text{Cl}(^2P_{3/2})$  causes  $\Gamma$  to decrease.

We can understand the  $J$  dependence of  $\Gamma$  in more detail by examining the diabatic state characters of the  $g_0$  state. The characters were calculated by adjusting the parameters in an effective Hamiltonian by a least-squares fit of the term values for all observed levels of Rydberg states with  $(X^2\Pi)4p\sigma$  and  $(X^2\Pi)4p\pi$  configurations.<sup>18</sup> The

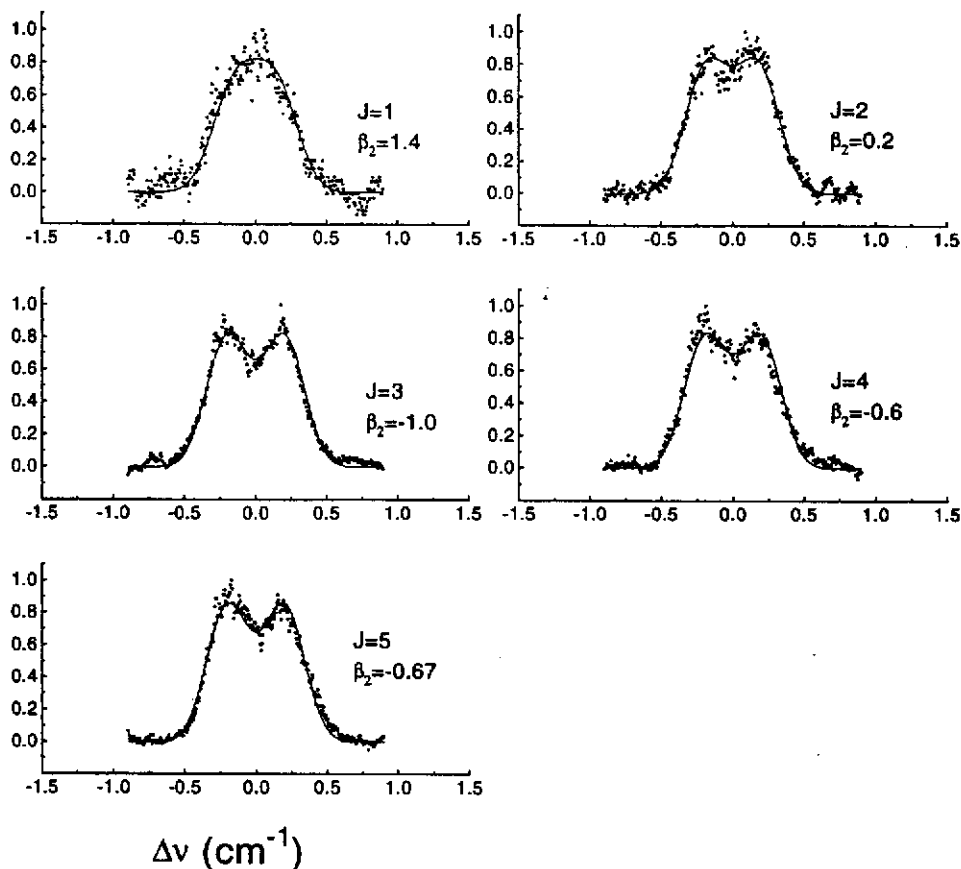


FIG. 5. Doppler profiles of  $\text{Cl}(^2P_{3/2})$  produced by predissociation of the  $g^3\Sigma_0^-$  state of HCl.

$C^1\Pi/b^3\Pi$  states were not included in this analysis because of the large uncertainty of the term values for the strongly predissociated, vibrationally excited levels. For the  $g_0$  state of DCl, the five leading contributors (accounting for  $\sim 98\%$  of the total state character) are  $g_0(v=0)$ ,  $E(v=0)$ ,  $g_1(v=0)$ ,  $V(v=13)$ , and  $V(v=14)$ . For  $J=1$ , the percent contributions of these states are 76, 20,  $<1$ ,  $<1$ , and  $<1$ . As shown in Fig. 6, the contribution of  $g_1$  increases monotonically with  $J$ , growing to 8% for  $J=8$ . A similar trend is observed for HCl in Fig. 7, for which the dominant diabatic contributions are from the  $g_0(v=0)$ ,  $E(v=0)$ ,  $g_1(v=0)$ , and  $V(v=9,10,11)$  states. Again the  $g_1$  character grows monotonically with  $J$ , increasing from 1% for  $J=1$  to 7% for  $J=5$ . The  $g_1$  state is more strongly predissociated than  $g_0$ , as is evident from the broad, diffuse lines that we observed for  $J=1-3$  of HCl. The decreasing values of  $\Gamma$  for the  $g_0$  state of HCl and DCl are therefore attributed to increased rotational coupling to the  $g_1$  state, which is in turn spin-orbit coupled to continuum states (or strongly predissociated states) that correlate with an excess of  $\text{Cl}(^2P_{3/2})$  atoms. The zero-order  $g_0$ ,  $E$ , and  $V$  states are spin-orbit coupled only to the  $a^3\Pi_0+$  continuum state [which gives mostly  $\text{Cl}(^2P_{1/2})$ ], whereas the zero-order  $g_1$  state is spin-orbit coupled to the  $a^3\Pi_1$ ,  $A^1\Pi$ , and  $t^3\Sigma_1^-$  continuum states, each of which correlates diabatically to a statistical distribution of  $\text{Cl}(^2P_J)$  states.

The observation that  $Y$  increases with  $J$  for the  $g_0$  state

of both HCl and DCl is readily explained by our finding that its  $g_1$  character increases with  $J$  for both isotopomers.

The photofragment anisotropy of the  $g_0$  state may be explained by the same coupling mechanism used to explain the  $J$  dependence of  $\Gamma$  and  $Y$ . Since a  $^3\Sigma_0^- \leftarrow ^1\Sigma^+$  transition is dipole forbidden, the  $g_0$  state must borrow its intensity

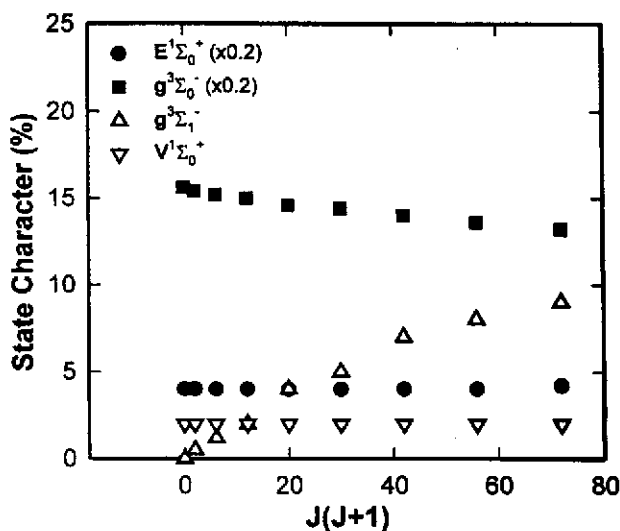


FIG. 6. Diabatic state character of the  $g^3\Sigma_0^-$  state of DCl. Note that the characters of the  $E$  and  $g_0$  states are multiplied by 0.2.

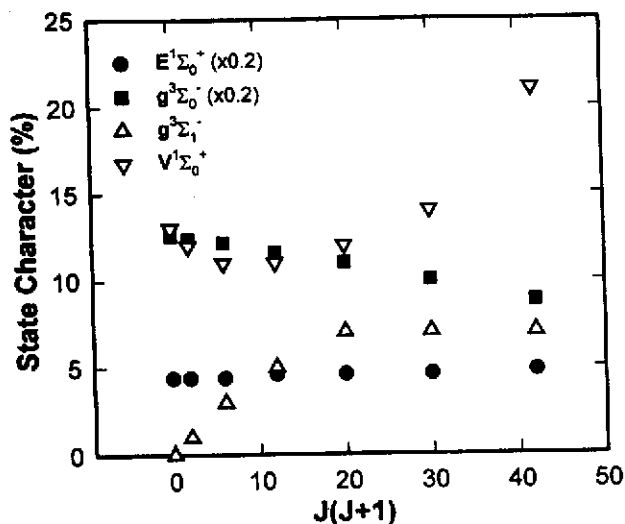


FIG. 7. Diatomic state character of the  $g^3\Sigma_0^-$  state of HCl. Note that the characters of the  $E$  and  $g_0$  states are multiplied by 0.2.

from other electronic states. For low  $J$  the obvious donor is the  $E^1\Sigma^+$  state. A two-photon  $\Sigma-\Sigma$  transition can occur through either a  $\Sigma$  or a  $\Pi$  intermediate state, the first resulting in a parallel-parallel transition, and the latter in a perpendicular-perpendicular transition. The actual path for a two-photon  $Q$ -branch is a coherent sum over many possible paths:  $(P,R)+(R,P)$  transitions for the intermediate  $\Sigma$  state and  $(Q,Q)+(P,R)+(R,P)$  transitions for the intermediate  $\Pi$  state.<sup>19</sup> From the two-photon absorption coefficient<sup>19</sup> (which is an integral over all recoil angles) it is impossible to determine uniquely the relative contributions of the possible paths,<sup>20</sup> whereas from the Doppler data we see immediately that the parallel-parallel paths dominate at low  $J$ . As  $J$  increases, oscillator strength is borrowed from a predissociating state with perpendicular alignment. The obvious choice is the strongly predissociated  $g_1$  state, which must be spin-orbit coupled to some other state with  $\Pi_1$  character. The most likely candidates are the  $C^1\Pi/b^3\Pi_1$  states,<sup>21</sup> which are also responsible for the intensity anomaly in the  $F^1\Delta$  state.<sup>5</sup> The absence of  $g_1$  character in the  $E$  state<sup>18</sup> is consistent with the  $J$ -independent behavior of this state.

In conclusion, we have shown how the diverse and divergent dynamical behaviors of two Rydberg states belonging to the same zero-order electronic configuration can be explained by their diabatic state characters. In the case of the  $E^1\Sigma^+$  state, strong Rydberg-valence interaction at the  $2\omega$  level leads to predissociation at the  $3\omega$  level. The extent of mixing, and hence the rate of predissociation, is  $J$  dependent, but the branching ratio and angular anisotropy of the fragments is  $J$  independent. The  $g^3\Sigma_0^-$  state obtains all of its oscillator strength from other states. The  $g^3\Sigma_1^-$  state carries perpendicular oscillator strength (via a  $^1\Pi$ ) state, and it is also more strongly predissociated than  $g_0$ . Consequently, the

$g_0-g_1$  interaction introduces new transition character ( $\beta_2$ ), different product branching ( $\Gamma$ ), and an increased dissociation rate ( $Y$ ). These findings illustrate the more general idea that a global understanding of both the spectroscopy and dynamics of a molecule may be obtained from a simple, effective Hamiltonian model.

## ACKNOWLEDGMENT

We thank the National Science Foundation for its generous support.

- H. Lefebvre-Brion and R. W. Field, *Perturbations in the Spectra of Diatomic Molecules* (Academic, New York, 1986).
- S. G. Tilford and M. L. Ginter, *J. Mol. Spectrosc.* **40**, 568 (1971).
- P. J. Dagdigian, D. F. Varley, R. Liyanage, R. J. Gordon, and R. W. Field, *J. Chem. Phys.* **105**, 10251 (1996).
- R. Liyanage, Y. Yang, S. Hashimoto, R. J. Gordon, and R. W. Field, *J. Chem. Phys.* **103**, 6811 (1995).
- R. Liyanage, P. T. A. Reilly, Y.-A. Yang, R. J. Gordon, and R. W. Field, *Chem. Phys. Lett.* **216**, 554 (1993).
- Y. Xie, P. T. A. Reilly, S. Chilukuri, and R. J. Gordon, *J. Chem. Phys.* **95**, 854 (1991).
- S. Arepalli, N. Presser, D. Robie, and R. J. Gordon, *Chem. Phys. Lett.* **118**, 88 (1985).
- W. C. Wiley and I. H. McLaren, *Rev. Sci. Instrum.* **26**, 1150 (1955).
- J. Zhang, M. Dulligan, and C. Wittig, *J. Chem. Phys.* **107**, 1403 (1987).
- For the transitions used to detect Cl atoms in this study, the ionization efficiency of  $\text{Cl}(^2P_{1/2})$  is taken to be 0.62 times the ionization efficiency of  $\text{Cl}(^2P_{3/2})$ . In Ref. 4 a calibration factor of 0.85, based on the measurements of Matsumi *et al.* [*J. Chem. Phys.* **97**, 5261 (1992)] was used, which led to systematically lower values of  $\Gamma$ .
- Z. Xu, B. Koplitz, and C. Wittig, *J. Chem. Phys.* **87**, 1062 (1987); **90**, 2692 (1989).
- R. N. Dixon, J. Nightingale, C. M. Western, and X. Yang, *Chem. Phys. Lett.* **151**, 328 (1988).
- R. J. Gordon and G. E. Hall, in *Advances in Chemical Physics*, edited by I. Prigogine and S. A. Rice, (Wiley, New York, 1996), Vol. 96, pp. 1-50.
- R. Liyanage and R. J. Gordon, *J. Chem. Phys.* **107**, 7209 (1997). The semiclassical model ignores exit channel effects and assumes that the angular distribution of the fragments mimics the alignment of the excited molecule. We used here the  $\beta_2$  value for a  $Q$ -branch of a  $\Sigma-\Pi$  transition, which is assumed to be responsible for the splitting in  $D(w/v)$ .
- The explanation of the  $J$ -dependent fragmentation of the  $E$  state is that the superexcited state reached from the zero-order  $V$  state dissociates faster than it autoionizes because it has an  $A^2\Sigma^+$  core, whereas the superexcited state reached from the  $E$  state can ionize directly. The ratio of ionization to predissociation is determined, therefore, by the amount of valence-Rydberg mixing at the  $2\omega$  level.
- Y. Matsumi, K. Tonokura, M. Kawasaki, and T. Ibuki, *J. Chem. Phys.* **93**, 7981 (1990).
- M. H. Alexander, B. Pouilly, and T. Duhoo, *J. Chem. Phys.* **99**, 1752 (1993).
- R. Liyanage, R. J. Gordon, and R. W. Field (unpublished).
- A. C. Kummel, G. O. Sitz, and R. N. Zare, *J. Chem. Phys.* **85**, 6874 (1986).
- T. F. Hansico and A. C. Kummel, *J. Phys. Chem.* **95**, 8565 (1991).
- Although the  $2+1$  REMPI signal for the  $C$  state is much weaker than that for the  $E$  state, its oscillator strength could be much larger than that of the  $E$  state. We observed that the width of the  $C-X(0,0)Q(1)$  transition of HCl is  $\sim 25$  greater than that of the corresponding  $E$  state transition. For both states the predissociation rate is much larger than the ionization rate. We estimate from the linewidths that the predissociation rate of the  $C(v=0, J=1)$  level is  $\sim 25$  times greater than the corresponding level of the  $E$  state. These two factors combine to reduce the REMPI signal for the  $C$  state by 2-3 orders of magnitude.